Enhanced thermoelectric properties in graphene nanoribbons by resonant tunneling of electrons

F. Mazzamuto,[1,*] V. Hung Nguyen,[1,2] Y. Apertet,[1] C. Caër,[1] C. Chassat,[1] J. Saint-Martin,[1] and P. Dollfus[1]

[1]*Institute of Fundamental Electronics, Université Paris-Sud, CNRS, UMR 8622, Orsay, France*

[2]*Institute of Physics, Vietnamese Academy of Science and Technology, Hanoi, Vietnam*

(Received 30 March 2011; published 29 June 2011)

Strongly enhanced thermoelectric properties are predicted for graphene nanoribbons (GNRs) with optimized pattern. By means of nonequilibrium Green's function atomistic simulation of electron and phonon transport, we analyze the thermal and electrical properties of perfect GNRs as a function of their width and their edge orientation to identify a strategy likely to degrade the thermal conductance while retaining high electronic conductance and thermopower. An effect of resonant tunneling of electrons is detected in mixed GNRs consisting of alternate zigzag and armchair sections. To fully benefit from this effect and from strongly reduced phonon thermal conductance, a structure with armchair and zigzag sections of different widths is proposed. It is shown to provide a high thermoelectric factor of merit *ZT* exceeding unity at room temperature.

DOI: 10.1103/PhysRevB.83.235426 PACS number(s): 61.48.Gh, 65.80.Ck, 72.80.Vp

I. INTRODUCTION

The discovery of two-dimensional graphene and quasi-one-dimensional graphene nanoribbons (GNRs) has led to a renewed interest in carbon-based materials to take advantage of remarkable physical properties with high potential for innovative applications in nanoelectronics, spintronics, photonics, and optoelectronics.[1–7] Recently, much attention has been focused on thermal[8] and thermoelectric[9] properties of graphene structures. For a two-dimensional graphene sheet, a giant Seebeck coefficient has been predicted,[10] and an extremely high thermal conductivity of about 5 $kW{\cdot}m^{-1}{\cdot}K^{-1}$ has been measured.[11] Additionally, the phonon contribution to thermal conductivity is expected to be strongly dependent on the GNR structure and significantly reduced by edge disorder at some specific phonon frequencies, which provides the possibility of designing devices with specific temperature dependence of the thermal conductivity.[12] Such promising results have oriented many works toward thermoelectric properties in GNRs.[13] Recently, it has been predicted that the thermoelectric figure of merit *ZT* can exceed unity in honeycomb chains of carbon atoms[14] and also in long rough-edge GNRs[15] or in GNRs with atom vacancies.[16] However, detailed information on the potential of short GNRs to provide a high figure of merit *ZT* at room temperature in ordered structures is still missing.

In this article, we analyze the influence of the GNR lattice structure on the electron and phonon transport with a view to identify a strategy making it possible to achieve good thermoelectric properties and in particular a high thermoelectric factor of merit *ZT* defined as $ZT \equiv TG_eS^2/\kappa$, where G_e is the electronic conductance, *S* is the thermopower (or Seebeck coefficient) and $\kappa = \kappa_e + \kappa_{ph}$ is the thermal conductance composed of electron and phonon contributions κ_e and κ_{ph}, respectively. On the basis of results obtained for elementary GNR structures, the strategy consists of designing specific structures where the phonon transmission and thus the thermal conductance are degraded, while the electronic conductance and the thermopower are still high or even enhanced. We will show that these objectives may be reached by alternating GNR slices of different widths and edge orientations, which strongly reduces the thermal conductance and gives rise to an effect of resonant tunneling of electrons. Such resonant effect has been recently predicted for GNR structures combining armchair-edge graphene nanoribbons (AGNRs) of different width.[17] Taking advantage of this phenomenon and from strongly reduced phonon thermal conductance, *ZT* values exceeding unity are then achieved at room temperature.

To fabricate these structures, the technological challenge of controlling precisely the ribbon edges at the atomic scale is expected to be overcome soon. Rapid progress in technology has been achieved in this direction. Recently, Li *et al.*[18] successfully fabricated very regular-edge ribbons of sub-10 nm width using chemical methods and self-assembly processes. Tapaszto *et al.*[19] used the scanning tunneling microscopy to pattern different shapes of graphene ribbons with nanometer precision. Very recently, Masubuchi *et al.*[20] used the tapping-mode atomic force microscopy and successfully demonstrated ribbons with well-controlled edge shapes.

II. MODEL AND METHODOLOGY

For the simulation of charge transport in graphene devices, the most widely used approach is based on the powerful nonequilibrium Green's function (NEGF) formalism to treat either the continuous Dirac Hamiltonian in 2D graphene sheets[21,22] or an atomistic tight-binding Hamiltonian in GNRs.[23–28] Different semiclassical and quantum approaches have been developed for phonon transport, such as molecular dynamics,[29] transfer matrix[12] or even NEGF[30] and real-space Kubo[31] approaches. Recently, the investigation of the thermoelectric properties in GNR structures has been performed within the NEGF formalism to calculate both the electron and the phonon transmissions on an equal footing.[13,15,32] In most of these works, a simple nearest-neighbor tight-binding (NNTB) Hamiltonian without edge relaxation was used for electrons, while a force constant model (FCM) including the fourth nearest neighbors[15,32] was considered for phonons.

In this work, a phonon Hamiltonian based on a fifth nearest-neighbor FCM[33] and an NNTB electron Hamiltonian including armchair edges relaxation fitted from first-principle calculation[27,34,35] were used. It has been shown that the average bond length in GNRs and graphene nanoflakes (GNFs) rapidly converge to the average bond length of a relaxed sheet of

graphene when increasing the number of atoms.[36] However, *ab initio* simulations have demonstrated that the relaxation of armchair edges significantly changes the edge bond length and tight-binding parameters.[37,38] This effect has been predicted to be much smaller for zigzag edge bonds.[39] In our work the bond relaxation is included using two different tight-binding (TB) parameters: the hopping energy of 3.02 eV is used for armchair edge bonds;[27] and the standard value of 2.7 eV is used for internal and zigzag edge bonds as in relaxed 2D graphene. More accurate models, including up to the third nearest neighbors could be considered,[40] but it is expected that this simple and computationally efficient approach provides relevant results. It is important to note that for the AGNRs which are found to be metallic when using a single hopping parameter, a small band gap opens when considering the edge relaxation through a specific edge- hopping parameter. In what follows, such AGNRs will be termed quasimetallic.

Due to the weak electron-phonon coupling in GNRs,[41] in our approach both phonon and electron populations are assumed to travel ballistically and independently. The electron (phonon) transmission function $T_{e(ph)}$ is calculated according to the NEGF formalism. The anharmonicity of atomic interactions is neglected in our calculation. Once the transmission functions are known, the Landauer formalism can be applied to calculate phonon and electron fluxes.[42] Finally, the thermopower S and the electronic contribution to the thermal conductance κ_e are calculated as detailed in Refs. 34 and 43. The surface Green's functions and the device Green's functions are calculated using the fast iterative scheme proposed in Ref. 44 and the recursive algorithm described in Ref. 45, respectively.

The ribbons presented in Fig. 1 are defined by their edge orientations and by the number n of dimers in the unit cell, which is related to the ribbon width W. In this article three types of ribbons are considered: GNRs with armchair, zigzag, and mixed edges are denoted by n-AGNR, n-ZGNR, and n-MGNR, respectively. The MGNR edges can be seen as a mixture of both armchair and zigzag edges in the elementary cell, which, as the chirality of a carbon nanotube, may be fully characterized by a couple of numbers, giving the numbers of AGNR and ZGNR elementary cells, respectively, in the MGNR unit cell.

The simulated structures are schematized in Fig. 1. They all consist of a GNR active zone coupled with two semi-infinite contacts with the same structure.

To identify a strategy to optimize the thermoelectric performance, we first examine the influence of GNR width and edge orientation on electron and phonon transport properties.

III. INFLUENCE OF GNR WIDTH AND ENERGY GAP

In Fig. 2 the electronic conductance G_e, the Seebeck coefficient S, and the factor of merit ZT are compared as a function of the chemical potential for several n-AGNRs exhibiting either a quasimetallic behavior with a narrow conductance gap ($n = 8$, 17, and 32) or a semiconducting behavior ($n = 16$). First, it is worth noting that the ZT peak positions correspond exactly to the electronic conductance transitions from one step to another. Though these results were achieved at room temperature, this observation is fully

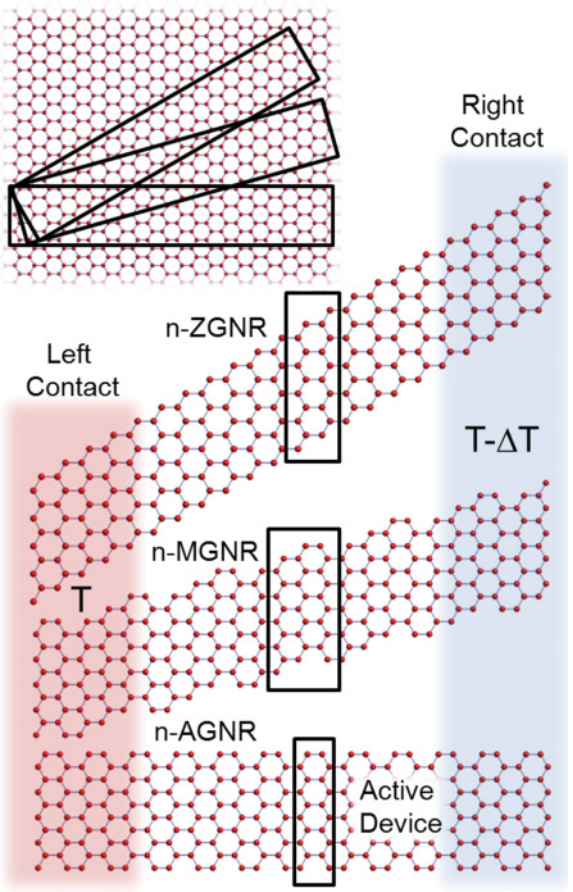

FIG. 1. (Color online) Simulated GNR structures with different edge orientations.

consistent with the Cutler–Mott theory $\{S \propto d[\ln(G_e)]/dE\}$ established at low temperature.[46] As expected, if the AGNR width, i.e. the number n, is reduced, the phonon thermal conductance reduces, too, and the band gap broadens, both for quasimetallic and semiconducting ribbons. For instance, for the quasimetallic AGNRs, the electronic band gap increases from 70 meV for 32-AGNR to 200 meV for 8-AGNR, and the phonon thermal conductance reduces from about 4.8 nW/K to 1 nW/K, as shown in Fig. 2(b). Though both phonon and electron contributions to the thermal conductance are included in the calculation of ZT, only the latter is plotted here. Indeed, it has been shown that in GNRs with perfect edges the phonon contribution is at least one order of magnitude higher than the electron contribution.[34] However, it is not true for all GNRs studied in this letter, which will be discussed later. Additionally, the theoretical prediction of a linear relationship between the maximum value of the Seebeck coefficient and the energy band gap of a semiconductor[47] is actually observed here, as shown in the inset of Fig. 2(c). It gives a strong advantage to the semiconducting 16-AGNR in terms of thermopower. However, this advantage is not strong enough to get a high value of ZT. Indeed, the quasimetallic 8-AGNR benefits from a smaller thermal conductance and a higher maximum power factor S^2G_e to provide a higher ZT value than 16-AGNR [Fig. 2(d)]. Regarding the influence of GNR width, it is observed that the maximum ZT value is

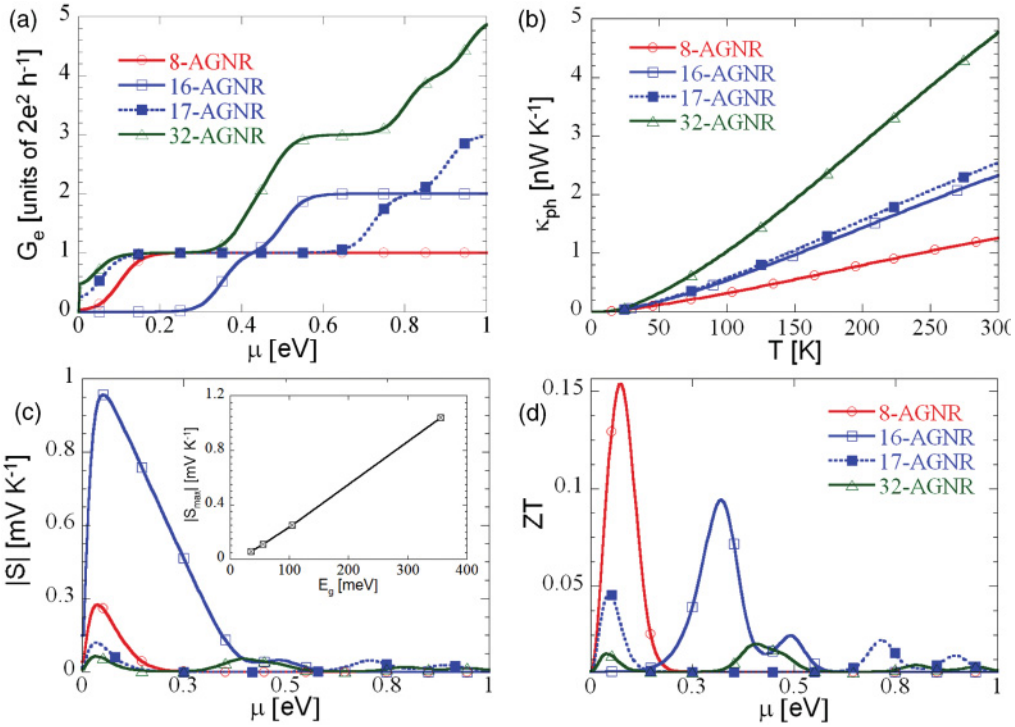

FIG. 2. (Color online) Width-dependence of (a) electronic conductance, (c) Seebeck coefficient, and (d) factor of merit ZT as a function of the chemical potential μ by comparison of 8-AGNR, 16-AGNR, 17-AGNR, and 32-AGNR. (b) Phonon thermal conductance as a function of the temperature for the same GNRs. The origin of the chemical potential is taken at the midgap position. Inset of (c) is the maximum absolute value of thermopower as a function of the energy gap.

improved by one order of magnitude when the ribbon width is divided only by four.

IV. INFLUENCE OF EDGE ORIENTATION

We now investigate the influence of GNR edge orientation on thermoelectric properties by considering GNRs of similar width. In Fig. 3 the quantities G_e, S, and ZT are plotted as a function of the chemical potential for 16-AGNR, 17-AGNR, 16-ZGNR, and for two 16-MGNRs of different chirality, while κ_{ph} is plotted as a function of temperature. ZGNRs are always gapless and AGNRs have an n-dependent band gap width. As shown in Fig. 3(b), in spite of their structural differences, perfect AGNRs and ZGNRs with the same number of dimers in the elementary cell have a similar thermal conductance. However, the semiconducting, quasimetallic, or metallic characters lead to very different thermoelectric properties, even with equivalent thermal conductance. While the metallic 16-ZGNR exhibits a poor thermopower and a very small ZT factor of merit [not even visible in Fig. 3(d)], the presence of a band gap in the semiconducting 16-AGNR leads to rather significant thermopower and ZT values, more than one order of magnitude higher than in 16-ZGNR. It should be mentioned that though the 16-ZGNR has a physical width $\sqrt{2}$ times smaller than that of the 16-AGNR, it exhibits a slightly higher thermal conductivity, which is also detrimental to ZT.

Thermoelectric results for MGNRs with different chirality must be interpreted differently. Armchair edges induce a band gap opening, while zigzag edges generate gapless edge localized states, which has been verified experimentally.[48] The presence in the same elementary cell of both types of edges gives rise to very specific electron transport properties. Indeed, the ribbon sections with armchair edges can be seen as barriers between localized zigzag edge states, and an MGNR can be seen as a multibarrier system. Thus, as predicted in Refs. 46 and 49 for multibarrier systems, a resonant tunneling transport may occur and induce strong oscillations of thermopower and electronic conductance. If the armchair edge sections are short, e.g. for chirality (1,1), the band gap is very small, and the MGNR has a metallic behavior similar to that of a perfect ZGNR. On the other hand, if the length of armchair sections is higher than that of the zigzag ones, the band gap broadens, and the resonant tunneling phenomenon becomes dominant. Figure 3(a) shows that an energy band gap of 300 meV is formed in the electronic conductance of the MGNR (5,1), and the resonant tunneling effect manifests in this structure through the oscillations of the conductance. Since the thermopower is related to the derivative of the electronic conductance, the negative differential conductance associated with the resonant effect gives rise to oscillations of the thermopower between negative and positive values [Fig. 3(c)], which is typical of a multibarrier system. To illustrate this resonant effect, the atomic local density of states (LDOS) are plotted in Fig. 4(a) for the electron energies E of 0.65 eV and 0.3 eV, corresponding to the first two maxima of electronic conductance. Consistent with recent experimental results,[48] the electron density is strongly localized at the zigzag edges. In this 16-MGNR working in the resonant tunneling regime, the electron conduction is perfect at $E =$ 0.3 eV, while it is weak in the corresponding 16-AGNR.

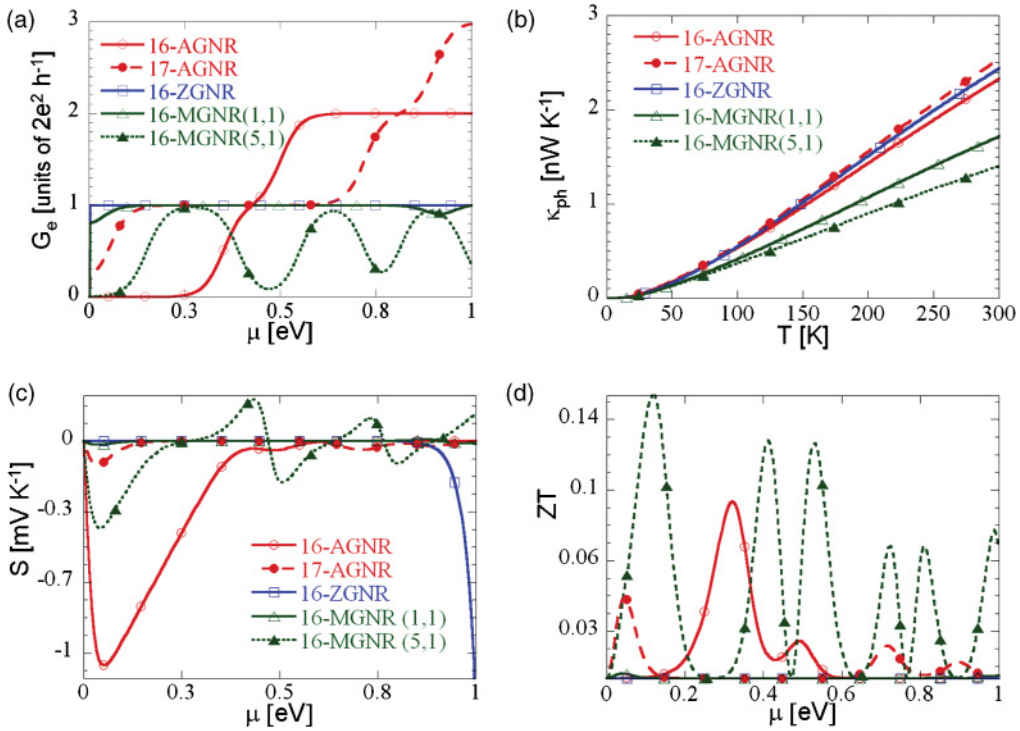

FIG. 3. (Color online) Edge-dependence of (a) electronic conductance G_e, (c) Seebeck coefficient, and (d) factor of merit ZT as a function of the chemical potential μ by comparison of 16-AGNR, 17-AGNR, 16-ZGNR, 16-MGNR with chirality (1,1), and 16-MGNR with chirality (5,1). (b) Phonon contribution to the thermal conductance as a function of the temperature for the same GNRs.

In contrast, the conduction vanishes at $E = 0.45$ eV, while it is high in both 16-AGNR and 16-ZGNR. In Fig. 4(b), the LDOS averaged along the ribbon width is shown as a function of both the distance along the structure and the electron energy. The energy gaps of the density of states (DOS) are of course in accordance with the energy gaps of the conductance resulting from the resonant tunneling effect.

In addition to this resonant tunneling effect, the MGNRs exhibit low thermal conductance because of the weak phonon transmission functions (not shown) compared to perfect AGNRs or ZGNRs [Fig. 3(b)]. This phenomenon was expected, since it results from the discrepancy between AGNR and ZGNR vibrational modes.[35,50] In particular, the specific phonon modes of AGNRs are suppressed in ZGNRs and vice versa. The thermal conductance at room temperature decreases from 2.5 nW/K for the perfect 16-AGNR to 1.4 nW/K for the 16-MGNR with chirality (5,1).

Finally, though GNRs with mixed edges exhibit moderate values of S, they can offer better thermoelectric performance than AGNRs. The maximum values of S are smaller in the 16-MGNR (5,1) than in the 16-AGNR of similar width

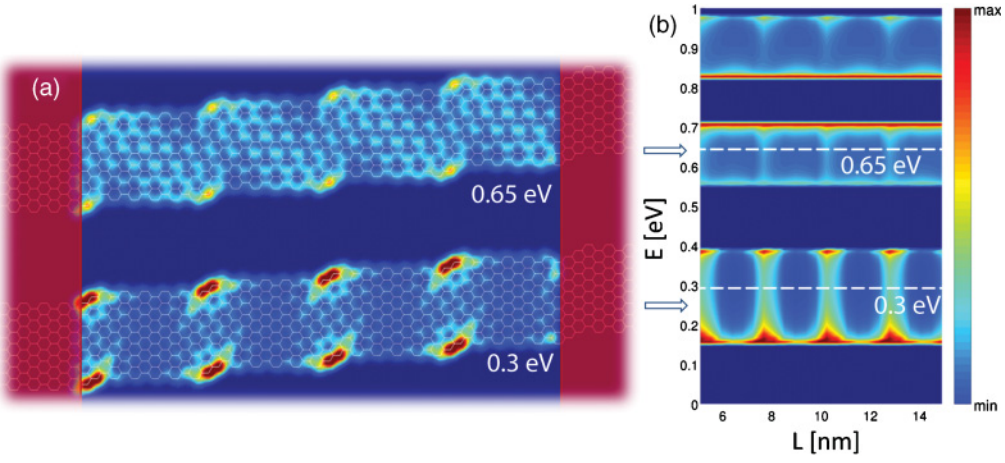

FIG. 4. (Color online) (a) Atomic LDOS of the 16-MGNR with chirality (5,1) calculated at the chemical potential of 0.65 eV and 0.3 eV. (b) Width-averaged LDOS map in the energy-length space.

[Fig. 3(c)], but the power factor S^2G_e is nearly the same in both GNRs (not shown), and thanks to the lower thermal conductance, the maximum value of ZT is higher in the MGNR than in the AGNR with several peaks due the resonant tunneling [Fig. 3(d)].

V. OPTIMIZED STRUCTURES

Now with a view to achieve a high ZT factor, we propose to design some optimized GNR structures likely to strengthen the resonant tunneling effect and to further degrade the thermal conductance. The strategy should follow two main principles: first, the structure must degrade the phonon transport; and second, it must enhance S without degrading G_e. Since it is established that a high energy band gap is desirable to achieve high thermopower values, the 8-MGNR with chirality (5,1) appears as a good candidate; it is the structure α in Fig. 5(a). The resonant effects in electronic conductance should be boosted by increasing the length of ZGNR elementary cells. The 8-MGNR with chirality (5,3) is thus proposed [structure β in Fig. 5(a)]. Consistently with Ref 32, the thermal conductance can be strongly degraded using two different widths in the elementary cell. A third solution is thus proposed. Starting from the 8-MGNR with chirality (5,3), the width of the ZGNR sections is increased. The structure consists in alternating 8-AGNR and 20-ZGNR sections, as shown in Fig. 5(a) (structure γ).

For the three structures, the electronic and thermal conductances, the Seebeck coefficient, and the factor of merit ZT are plotted in Figs. 5(b), 5(e), 5(c), and 5(d), respectively.

The structure α gives rise to a very limited resonant tunneling behavior with small oscillations of the electron conductance. In structure β these oscillations are more pronounced, but the phonon thermal conductance is similar. Additionally, because of a reduced band gap width, the maximum thermopower values are smaller. The resulting ZT values in the structure β are thus smaller than in the structure α.

However, in structure γ the localized states associated with zigzag edges strengthen the resonant effects. They induce a strongly selective electronic transmission which manifests through strong oscillations in the electronic conductance [Fig. 5(a)]. It is clearly illustrated in Fig. 6, where the atomic LDOS calculated at 0.05 eV and 0.3 eV [Fig. 6(a)] and the LDOS averaged over the width of the GNR [Fig. 6(b)] are shown together with the corresponding electron energy spectrum [Fig. 6(c)] and electron transmission [Fig. 6(d)] as a function of electron energy. The resonant character of the electronic transport can be fully understood if the electron energy spectrum is examined. The energy spectrum is determined by Bloch's theorem over the ribbon γ approximated to an infinite superlattice-like structure. In this mixed structure, we observe the building of energy gaps and minibands which are not present in perfect AGNRs and ZGNRs. It should be noted

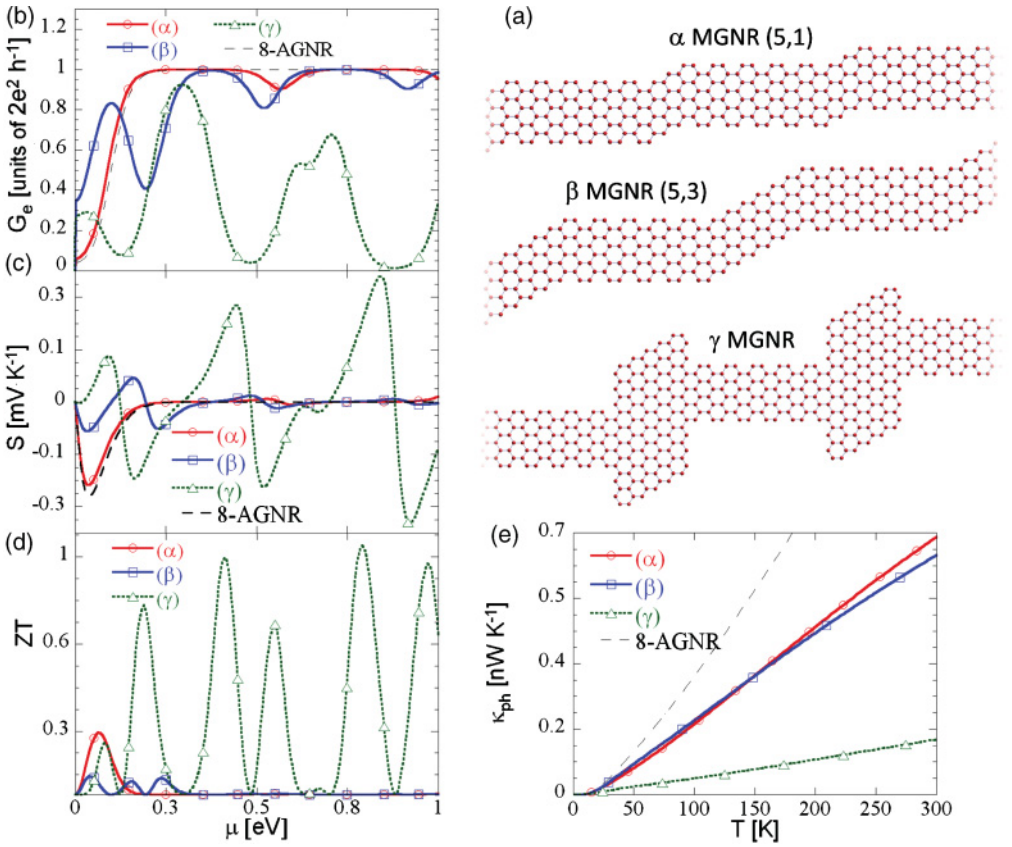

FIG. 5. (Color online) (a) MGNR alternating armchair and zigzag elementary cells with the same width (α and β) and with different widths (γ). (b) Electronic conductance, (c) Seebeck coefficient, (d) and factor of merit ZT as a function of chemical potential μ, (e) and phonon contribution to thermal conductance as a function of the temperature for different GNR structures.

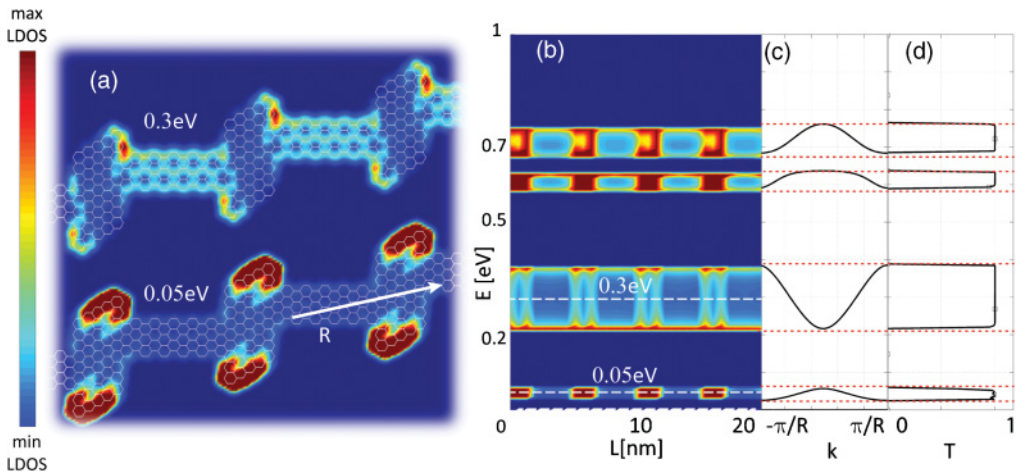

FIG. 6. (Color online) (a) The atomic LDOS calculated at 0.3 eV and 0.05 eV. (b) The corresponding width-averaged LDOS map in the energy-length space. (c) The electron energy spectrum as a function the momentum k along the ribbon. (d) The electronic transmission as a function of the electron energy.

that at the two energies 0.05 eV and 0.3 eV, corresponding to the first and second maxima of the electronic conductance, the distribution of localized electronic states is quite different. As a consequence of the strong resonant tunneling effect, the thermopower S is significantly enhanced with respect to structures α and β and exhibits strong oscillations from about -0.3 mV/K to 0.3 mV/K [Fig. 5(c)].

In parallel, the thermal conductance reduces drastically due to strong differences in phonon vibrational modes between the different sections of the ribbon, and it reaches a very low value <0.2 nW/K at room temperature [Fig. 5(e)]. It is worth noting that while the electron thermal conductance was negligible in AGNRs, ZGNRs, and even in MGNRs [Fig. 3], it is now comparable to the phonon thermal conductance (not shown), which is a consequence of the strong reduction of the latter. It is thus important to include the electron contribution to the thermal conductance in the calculation.

The combined effect of the thermopower enhancement and reduced thermal conductance finally boosts ZT, which exceeds unity for the structure γ at room temperature, as shown in Fig. 5(d). It is a remarkable result for possible applications of graphene in thermoelectrics.

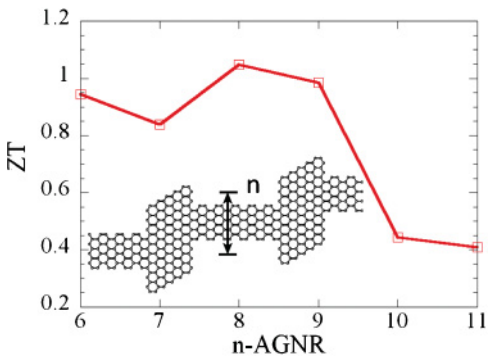

FIG. 7. (Color online) The value of the maximum ZT as a function of the number of dimers n in armchair sections in the structure γ of Fig. 5.

For the structure γ we now consider different width of the AGNR sections. In Fig. 7 the maximum figure of merit ZT is plotted as a function of the number of dimers in the AGNR elementary cell. The maximum ZT has been reached for about 8–9 dimers, and this parameter ZT decreases for larger AGNR sections. We did not analyze GNR of width $n < 6$ because a strong relaxation of all carbon bonds is expected and cannot be considered here.

VI. CONCLUSION

In summary, a specific patterning of a mixed GNR obtained by alternating armchair and zigzag sections of different width has been shown to provide high thermoelectric performance with a ZT factor reaching unity at room temperature. It results from the combination of (i) very small phonon thermal conductance due to the mismatch of phonon modes in the different sections and (ii) the resonant tunneling of electrons between these sections, which retains high electron conductance and thermopower. It should be noted that only intrinsic properties of suspended GNR structures have been explored in this work. To be inserted in a real thermoelectric device, the GNR should be deposited on a substrate and coupled with heat and electron reservoirs, which may strongly change the results. A first way to assess the relevance of the proposed design for thermoelectric conversion could be to simulate a full device, including reservoirs. It is certainly a valuable objective of future works.

ACKNOWLEDGMENTS

This work was supported in part by the French Agency ANR through Grant NANOSIM_GRAPHENE (ANR-09-NANO-016). We are grateful to Van Lien Nguyen, Arnaud Bournel, Vincent Talbo, Van Nam Do and Damien Querlioz for useful discussions. V.H.N. acknowledges Vietnam's National Foundation for Science and Technology Development for financial support under the Project No. 103.02-2010.33.

*fulvio.mazzamuto@u-psud.fr

[1] A. K. Geim and K. S. Novoselov, Nat. Mater. **6**, 183 (2007).
[2] A. H. Castro Neto, F. Guinea, N. M. R. Peres, K. S. Novoselov, and A. K. Geim, Rev. Mod. Phys. **81**, 109 (2009).
[3] A. K. Geim, Science **324**, 1530 (2009).
[4] F. Schwierz, Nat. Nanotechnol. **5**, 487 (2010).
[5] O. V. Yazyev and S. G. Louie, Nat. Mater. **9**, 806 (2010).
[6] F. Bonaccorso, Z. Sun, T. Hasan, and A. Ferrari, Nat. Photonics **4**, 611 (2010).
[7] N. Tombros, C. Jozsa, M. Popinciuc, H. T. Jonkman, and B. J. van Wees, Nature **448**, 571 (2007).
[8] A. A. Balandin, S. Ghosh, W. Bao, I. Calizo, D. Teweldebrhan, F. Miao, and C. N. Lau, Nano Lett. **8**, 902 (2008).
[9] Y. M. Zuev, W. Chang, and P. Kim, Phys. Rev. Lett. **102**, 096807 (2009).
[10] D. Dragoman and M. Dragoman, Appl. Phys. Lett. **91**, 203116 (2007).
[11] S. Ghosh, I. Calizo, D. Teweldebrhan, E. P. Pokatilov, D. L. Nika, A. A. Balandin, W. Bao, F. Miao, and C. N. Lau, Appl. Phys. Lett. **92**, 151911 (2008).
[12] L.-P. Shi and S.-J. Xiong, Phys. Lett. A **373**, 563 (2009).
[13] Y. Ouyang and J. Guo, Appl. Phys. Lett. **94**, 263107 (2009).
[14] X. Ni, G. Liang, J.-S. Wang, and B. Li, Appl. Phys. Lett. **95**, 192114 (2009).
[15] H. Sevinçli and G. Cuniberti, Phys. Rev. B **81**, 113401 (2010).
[16] T. Ouyang, Y. P. Chen, K. K. Yang, and J. X. Zhong, Europhys. Lett. **88**, 28002 (2009).
[17] H. Teong, K.-T. Lam, S. B. Khalid, and G. Liang, J. Appl. Phys. **105**, 084317 (2009).
[18] X. Li, X. Wang, L. Zhang, S. Lee, and H. Dai, Science **319**, 1229 (2008).
[19] L. Tapaszto, G. Dobrik, P. Lambin, and L. P. Biro, Nat. Nanotechnol. **3**, 397 (2008).
[20] S. Masubuchi, M. Ono, K. Yoshida, K. Hirakawa, and T. Machida, Appl. Phys. Lett. **94**, 082107 (2009).
[21] V. N. Do, V. H. Nguyen, P. Dollfus, and A. Bournel, J. Appl. Phys. **104**, 063708 (2008).
[22] Y. Ouyang, P. Campbell, and J. Guo, Appl. Phys. Lett. **92**, 063120 (2008).
[23] G. Fiori and G. Iannaccone, IEEE Electron Device Lett. **28**, 760 (2007).
[24] D. Gunlycke, D. A. Areshkin, and C. T. White, Appl. Phys. Lett. **90**, 142104 (2007).
[25] G. Liang, N. Neophytou, M. S. Lundstrom, and D. E. Nikonov, J. Appl. Phys. **102**, 054307 (2007).
[26] V. H. Nguyen, V. N. Do, A. Bournel, V. L. Nguyen, and P. Dollfus, J. Appl. Phys. **106**, 053710 (2009).
[27] P. Zhao, J. Chauhan, and J. Guo, Nano Lett. **9**, 684 (2009).
[28] G. Liang, N. Neophytou, M. S. Lundstrom, and D. E. Nikonov, Nano Lett. **8**, 1819 (2008).
[29] J. Hu, X. Ruan, and Y. P. Chen, Nano Lett. **9**, 2730 (2009).
[30] J. Lan, J.-S. Wang, C. K. Gan, and S. K. Chin, Phys. Rev. B **79**, 115401 (2009).
[31] W. Li, H. Sevinçli, G. Cuniberti, and S. Roche, Phys. Rev. B **82**, 041410 (2010).
[32] Y. Chen, T. Jayasekera, A. Calzolari, K. W. Kim, and M. B. Nardelli, J. Phys. Condens. Matter **22**, 372202 (2010).
[33] M. Mohr, J. Maultzsch, E. Dobardžić, S. Reich, I. Milošević, M. Damnjanović, A. Bosak, M. Krisch, and C. Thomsen, Phys. Rev. B **76**, 035439 (2007).
[34] F. Mazzamuto, V. H. Nguyen, V. N. Do, C. Caer, C. Chassat, J. Saint-Martin, and P. Dollfus, in Proc. Computational Electronics (IWCE), 14th International Workshop on, 1–4 (2010).
[35] F. Mazzamuto, J. Saint-Martin, A. Valentin, C. Chassat, and P. Dollfus, J. Appl. Phys. **109**, 064516 (2011).
[36] A. S. Barnard and I. K. Snook, J. Chem. Phys. **128**, 094707 (2008).
[37] Y.-W. Son, M. L. Cohen, and S. G. Louie, Phys. Rev. Lett. **97**, 216803 (2006).
[38] Y.-W. Son, M. L. Cohen, and S. G. Louie, Phys. Rev. Lett. **98**, 089901 (2007).
[39] Q. Lu and R. Huang, Phys. Rev. B **81**, 155410 (2010).
[40] D. Gunlycke and C. T. White, Phys. Rev. B **77**, 115116 (2008).
[41] D. Gunlycke, H. M. Lawler, and C. T. White, Phys. Rev. B **75**, 085418 (2007).
[42] Y. Imry and R. Landauer, Rev. Mod. Phys. **71**, S306 (1999).
[43] U. Sivan and Y. Imry, Phys. Rev. B **33**, 551 (1986).
[44] M. P. L. Sancho, J. M. L. Sancho, and J. Rubio, J. Phys. F **14**, 1205 (1984).
[45] M. P. Anantram, M. S. Lundstrom, and D. E. Nikonov, Proc. IEEE **96**, 1511 (2008).
[46] G. D. Guttman, E. Ben-Jacob, and D. J. Bergman, Phys. Rev. B **51**, 17758 (1995).
[47] H. Goldsmid and J. Sharp, J. Electron. Mater. **28**, 869 (1999).
[48] K. A. Ritter and J. W. Lyding, Nat. Mater. **8**, 235 (2009).
[49] M. Larsson, V. B. Antonyuk, A. G. Mal'shukov, and K. A. Chao, Phys. Rev. B **68**, 233302 (2003).
[50] A. V. Savin, Y. S. Kivshar, and B. Hu, Phys. Rev. B **82**, 195422 (2010).